The spinning terrella plasma experiment: Initial results

Robert B. Sheldon and Scott Spurrier
Physics Department, The University of Alabama in Huntsville, Huntsville, Alabama 35899

(Received 9 August 2000; accepted 26 January 2001)

The observation of 40 keV field-aligned plasma flows (Sheldon *et al.*, 1998) has been conjectured as the result of a space-charge driven instability generating kV parallel potentials (Sheldon, 1999), which occur whenever hot plasma drifts in an inhomogeneous magnetic field. Such conditions occur in almost any magnetic field that interacts with an energetic plasma: at the Earth, the Sun, Jupiter, and perhaps even astrophysical magnetospheres of stars, black holes and active galactic nuclei, all of which possess collimated flows. From this ubiquity, field-aligned flows were looked for in a table top plasma experiment involving a permanent magnet and a direct current (dc) discharge source of energetic plasma. It is emphasized that a one-fluid plasma theory such as magnetohydrodynamics is incapable of describing a parallel potential drop, and that most second-order corrections to the theory predict weak parallel voltages proportional to the thermal energy. In contrast, it is shown photographs of the plasma and peculiar high-voltage ($500\ \mathrm{eV} \gg kT$) discharges suggestive of a large field-aligned potential drop. It is proposed that this may be a manifestation of the quasi-neutral catastrophe heretofore neglected by space and laboratory plasma physicists, which may unify many disparate observations. © *2001 American Institute of Physics.* [DOI: 10.1063/1.1355982]

I. INTRODUCTION

Theoretically, kV field-aligned potentials have been surprisingly hard to explain.[1,2] The highly successful formalism of magnetohydrodynamics (MHD), which generally works well on large magnetized plasma systems, completely excludes the possibility of field aligned potentials for the simple reason that electrons traveling along the field lines would be accelerated by such potentials and quickly redistribute the charge.[3] Second-order effects, such as polarization drifts have been shown to provide a very small parallel potential, but always on the order of the thermal energy of the electrons. Despite the very real observational data on parallel fields, theoretical explanations generally fall back on an *a priori* boundary condition, such as an externally imposed pitchangle distribution, or a large field-aligned current, or the presence of a specific wave model. One explanation for why all previous theoretical efforts have found so little quasi-static parallel potential may perhaps be related to their assumption of quasi-neutrality early in the calculation, and therefore they naturally find only small deviations from it.[4,5] The assumption is normally valid, because unshielded charge can create truly large voltages, so that a few Coulombs at the top of a thundercloud are thought to produce gamma rays![6]

However, the data are showing that large parallel voltages in plasmas do exist,[7,8] and have important consequences for both space physics and astrophysics, much as they do in meteorology. In space physics, we believe parallel potentials explain much of the phenomenology of a geomagnetic storm,[9] and are implicated as a source of the Earth's aurora.[1]

At the Sun, parallel potentials may be significant in coronal loops that flare and produce copious x rays.[10] At Jupiter, observations of beaming electrons near the orbit of Io implicate a parallel acceleration mechanism.[11] In astrophysics, the observation of highly collimated jets arising from rapidly spinning magnetic fields encircled by hot accretion disks are ubiquitous;[12] seen in young stellar objects (YSO), Herbig–Haro objects, microquasars, galaxies and active galactic nuclei (AGN). If these jets are all a result of parallel potentials, then we may have found a unifying theory to explain their mysterious origin. And since one would expect nonthermal x rays to be another signature of parallel potentials, it may be that the 50% of the near continuum of discrete sources of the x-ray background observed by Chandra[13] are all powered by such a mechanism.

The goal of this paper is to motivate the proposal that large parallel potentials can develop in a plasma by considering first space charge production in thunderstorms, then spacecraft data taken in the Earth's magnetosphere, followed by observations of astrophysical jets. Finally we present initial results of a tabletop laboratory experiment that is suggestive of the production of parallel potentials much larger than the few eV permitted by standard plasma theory.

II. THE QUASI-NEUTRAL CATASTROPHE

Since we are arguing that parallel potentials develop in a magnetized plasma due to space charge, it is instructive to ask how space charge forms in a thunderstorm. Some mechanism like friction separates charges which are subsequently attached to rain drops or ice crystals. The insulating atmosphere prevents the charges from immediately recombining, but as of yet they are quasi-neutral. Then a powerful energy source, wind or gravity, does work against the Coulomb force to separate the charge and store energy in the electric field. This process continues until the growing electric field causes an avalanche breakdown of the insulating air.[14] Thus by analogy, we are looking for an innocuous process in plasmas that separates charges, in a medium that prevents imme-

diate recombination, followed by a powerful energy source that drives these charges apart. All three steps are found in hot magnetized plasmas.

Consider a blob of hot neutral plasma that convects into an inhomogeneous magnetic field (e.g., a dipole) that is devoid of ambient plasma. ∇B drifts immediately separate the ions and electrons. A magnetized plasma has very low perpendicular conductivity, which prevent the ions and electrons from immediately recombining. Convection electric fields, set up by the fast rotation of the central magnet, play the part of the thunderstorm updrafts and contribute to large-scale separation of charges. Consequently, a large space charge builds up on a magnetic flux tube. This charge experiences a repulsive Coulomb force that would drive it deep into the central magnet (or ionosphere) but is constrained by the mirror force, leading to a steep, peaked space-charge potential at the mirror point.

If the non-neutral plasma is not to precipitate onto the central magnet, there must exist an equilibrium between the mirror force directed toward the equator and the space charge directed away from the equator such that

$$\mu_i \nabla_\parallel B = q_i \nabla_\parallel \Phi, \tag{1}$$

where B is the magnetic field strength, Φ is the electrostatic potential, q is the charge, and μ the magnetic moment of the ith particle. From the Poisson equation, the divergence of the electric field is

$$\nabla^2 \Phi = Q/4\pi\epsilon_0, \tag{2}$$

where Q is the charge enclosed by the flux tube. Combining equations yields

$$\frac{\mu_i}{q_i}\nabla_\parallel^2 B = \frac{Q}{4\pi\epsilon_0}. \tag{3}$$

Since the magnetic-field strength along a dipole field line weakens as $B(r) \propto r^{-3}$, where r is the distance from the central dipole, then the parallel electric field $E_\parallel = \nabla_\parallel \Phi \propto r^{-4}$, and the charge density $Q \propto r^{-5}$. Thus, starting at the equator on a field line where the mirror force and the parallel electric field are zero, the density of charge must monotonically increase as we move toward the ionosphere and our radius decreases. When this steeply rising density integrates to the total amount of injected charge, then the density abruptly goes to zero. Thus the space charge generated potential along a field line has a sharp, double-peaked structure, one peak at each mirror point on the field line.

Our initial assumption, that the injection of hot plasma occurs in a vacuum dipole field, is generally not the case at the Earth. Since it seems rather common that the vacuum dipole field is filled with a cold plasma, it is instructive to calculate the equilibrium electric field for a cold Maxwellian neutral plasma, and a hot ion ''beam'' having an arbitrary but specified pitchangle. This is the calculation done by Whipple,[5] which we summarize below.

A. Whipple's first equilibrium

Our initial populations can be described by a phase density for electrons and ions as follows:

$$f_e = n\left(\frac{m_e}{2\pi kT}\right)^{3/2} e^{(-K/kT)}, \tag{4}$$

$$f_i = (n-n_b)\left(\frac{m_e}{2\pi kT}\right)^{3/2} e^{(-K/kT)} + n_b/(\pi B_0) \times \left(\frac{m_e}{2}\right)^{3/2} K_b^{1/2}\,\delta(\mu-\mu_b)\,\delta(K-K_b), \tag{5}$$

where we specify the density of the beam as n_b, and the density of the cold plasma as n; the first invariant is μ; the beam value is μ_b; the total energy K; the beam energy K_b; and the cold plasma temperature, kT. Generalizing from Whipple's Eq. (18), we allow μ_b to take on values other than zero.

If we carry out the zeroth moment integral to find the quasi-neutrality condition according to the Whipple prescription, we arrive at a similar equation,

$$x \equiv q\Phi/kT, \tag{6}$$

$$K_\parallel \equiv K_b - \mu_b B, \tag{7}$$

$$r \equiv n_b/n, \tag{8}$$

$$e^x = (1-r)e^{-x} + \frac{rB}{B_0}\sqrt{\frac{K_\parallel}{K_\parallel - xkT}}. \tag{9}$$

By the appropriate asymptotic expansions, we can characterize the solution as a function of x. Let x be small and positive, corresponding to a few volt (few kT) potential needed to shift the thermal plasma such that the ion beam is neutralized.

$$e^x + (r-1)e^{-x} = \frac{rB}{B_0\sqrt{1-(xkT/K_\parallel)}}, \tag{10}$$

$$e^{2x} + 2r - 2 + (r-1)^2 e^{-2x} = \frac{r^2 B^2}{B_0^2(1-xkT/K_\parallel)}. \tag{11}$$

Taylor expanding the exponential and truncating gives

$$\left(1-\frac{xkT}{K_\parallel}\right)(1-2x+4x/r)\frac{B_0^2}{B^2} \cong 1, \tag{12}$$

$$\frac{B^2/B_0^2 - 1}{4/r - 2 - kT/K_\parallel} \cong x. \tag{13}$$

From this expansion, we see that when we are at the equator, $B/B_0 = 1$ and the potential is zero, as defined by Whipple. Furthermore, since $r < 1$ and $kT/(K_b - \mu_b B) \ll 1$ is positive, the denominator is always positive definite. Thus the potential quadratically increases with B/B_0 away from the equator, which means a proton will be confined to the equator, but an electron will be accelerated away from the equator. This solution produces the well-known potential of several kT along the field line[15] as documented by Whipple.[5] Heuristically, this is all the voltage needed to shift massive numbers of cold electrons to the ion mirror point and shield the ion charge.

B. Whipple's second equilibrium

A second solution is possible if one recognizes that the right-hand side (rhs) of Eq. (9) can be very large as $q\Phi \rightarrow (K-\mu B)$. In this case we need to expand the exponentials around $y \equiv (K_b - \mu_b B)/kT - x$ giving

$$e^{-y}e^{K_\parallel/kT} = (1-r)e^{y}e^{-K_\parallel/kT} + \frac{rB}{B_0}\sqrt{\frac{K_\parallel}{ykT}}, \tag{14}$$

$$\gamma \equiv e^{2K_\parallel/kT}, \tag{15}$$

$$\frac{r^2B^2K}{B_0^2kT} \cong y[\gamma + 2r - 2 + (r-1)^2/\gamma], \tag{16}$$

$$\frac{r^2B^2K}{B_0^2kT\gamma} \cong y = \frac{K_\parallel}{kT} - x, \tag{17}$$

where we have kept only first order in y. Since $\gamma \gg 1$, the first term in the denominator of the rhs of Eq. (16) is the only contributor. This leads to

$$x = \frac{K_\parallel}{kT}\left(1 - \frac{r^2B^2}{B_0^2}\exp(-2K_\parallel/kT)\right), \tag{18}$$

$$q\Phi \cong K_\parallel = (K_b - \mu_b B), \tag{19}$$

which is a good approximation since the last term is very small. Note that the potential is a strong function of the parallel energy of the ions, $K_\parallel = K_b - \mu_b B$, and vanishes not at the equator, but at the mirror point of the ions. One can heuristically understand this potential as a maximum at the equator to retard the speed of the ions, and thereby spread the distribution of ions more evenly along the field line rather than concentrate the distribution at the mirror points, (e.g., a square-wave spatial ion distribution that minimizes the self-energy). Since the potential can be offset by a scalar without loss of generality, we can select the offset to be the equatorial parallel energy, $K_b - \mu_b B_0$. If we then plug in this potential for the left-hand side (lhs) of Eq. (9) we retrieve a reasonable density of electrons at the equator, and an exponentially decreasing density as we move away from the equator. Once we have traveled a short distance from the equator, we find unshielded ions around the mirror points resulting in the establishment of a space charge potential.

The transition from solution 1 to solution 2 is rather abrupt, since the potential jumps from a few volts to a few kV discontinuously. That is, these are the only two static equilibrium potential solutions, so the intermediate potentials are dynamic, nonequilibrium voltages. One can understand these two states by considering the fate of the cold plasma in these two equilibria. After the initial appearance of hot ions on a particular flux tube, the first eV solution is initially found by the cold plasma, which attempts to shield the hot ions around their density spikes at the mirror point. When the flux tube runs out of cold electrons, occurring first near the equator, the potential rapidly jumps to the second solution as a wave of high space charge potential radiates outward from the equator where the hot ions are ''stripped'' of their shielding electrons.

We call this violation of quasi-neutrality the ''quasi-neutrality catastrophe'' (QNC). Note that in this second equilibrium the parallel electric field is opposed to the mirror force, and therefore attempts to exclude the ions from the equator. Integrating the electric field from the equator to the mirror point shows that the total potential drop, $\Phi \propto K_{0\parallel}$, where $K_{0\parallel}$ is the parallel component of the kinetic energy at the equator. In other words, QNC is a transducer converting parallel hot ion energy into parallel potential, which can be much larger than the cold electron thermal energy.

III. THE EARTH'S MAGNETOSPHERE

In a vacuum dipole field, this space charge is a stable equilibrium, however, at the Earth other plasmas respond to the space charge electric field. Plasma on neighboring flux tubes would experience a perpendicular polarization electric field force causing an $E \times B$ drift around the space charged flux tube. More important is the $E_\parallel$ acceleration given to plasma on the same field line, but earthward of this structure, that is, inside the hot ion mirror point. The first specie to respond is the lightest, the electrons. If the space charge were composed of ions, then electrons would be accelerated from the ionosphere toward this positive space charge. Their momentum, as well as the ''reverse Debye shielding effect''[16] in which an accelerated phase space distribution must decrease in density, cause an ''overshoot'' of the sharp peak in ions.

Timescales are essential in discussing any dynamic instability. The electrons, despite their speed, require several milliseconds to travel the several thousand kilometers from the ionosphere. Since neutral densities are virtually negligible at these altitudes, and since the plasma densities are also very small ($\sim 10^4$/cc), thermalization and trapping of the electrons in the vicinity of the ion spike also requires milliseconds to seconds to occur. Therefore, one can approximate the potential as a spike of positive potential surrounded by a distended cloud of hot electrons that overshoot.

The addition of a spike and an overshoot, we surmise, leads to a ''Mexican hat'' potential distribution, whose gradient gives opposing electric fields suggestive of a ''double layer.'' The double layer should be transient and vanish on an electron collision/scattering time scale if it were not for the differing ∇B drift speeds of the ions and the electrons, which depend on the sign of the charge and the perpendicular energy. Since the electrons have opposite sign and little perpendicular energy, having been accelerated only parallel to the field, the ions drift away from the electrons on a ~ 1 second time scale, and begin the process anew.

The electrons that have pitchangle scattered in the vicinity of the ions are left behind as the ions ∇B drift away, and find themselves not in the loss cone, but trapped in the magnetosphere. Now the fate of the electrons is similar to that of the ions that began the process, finding themselves in a space-charge potential that is driving them back into the ionosphere. For these pitch angle scattered electrons, however, the mirror force restrains them from precipitating, which is to say, some electrons have scattered out of the loss

cone to become trapped. This gives the ions and electrons sufficient time to scatter and form a neutral plasma, albeit one with $T_{\parallel} > T_{\perp}$.

The inner edge of the plasma sheet is one region of the magnetosphere that should be susceptible to QNC. Here, hot plasma is continually injected into the dipolar magnetosphere and ∇B drifts become important to the dynamics of the region, perhaps leading to the formation of double layers in the auroral acceleration region. Consequently, geomagnetic storms might be an extreme example of QNC since, during main phase, the separatrix between corotating and convecting plasma (the Alfvén layer) moves Earthward to as little as 2.5 Re.[17]

Simultaneous POLAR/CEPPAD observations of 40 keV ionospheric field aligned beams with convected 90 keV plasmasheet ions[8] during a geomagnetic storm led to the proposal of QNC. Sheldon and Spence found that the ratio of trapped ion energy to beaming ion energy was constant over many thousands of kilometers, indicating that the trapped ions are creating the 40 kV parallel potentials required to extract and accelerate the ionospheric species. As a check on the mechanism, we note that their trapped ion pitch-angle distribution show a distinct cliff between 40 and 50 degrees, which would correspond to the maximum $K_{0\parallel}$ for this population. Using 45° as a best estimated pitchangle, this predicts that exactly half the trapped ion energy is available to produce parallel potential and accelerate cold ionospheric ions toward the equator, which is consistent with the 40 keV ions actually measured. (A better calculation would require integration of the measured equatorial pitch-angle distribution to estimate the total potential drop, which would likely be smaller than our upper limit estimate above.)

This QNC instability, then provides a simple explanation for many features of geomagnetic storms seen during main phase including duskside Pc1 waves,[18] localized x rays,[19] ring current filling,[20] the rapid Dst enhancement,[21] the drop in average energy of ring current ions,[22] the O^+ enrichment,[22,23] its proportionality to Dst,[24] and the two time-constant recovery of Dst.[22]

IV. ASTROPHYSICAL JETS

Astrophysical jets are beautifully puzzling structures that have resisted comprehensive theoretical interpretation despite 30 years of observation. The bottom panel of Fig. 1 presents a Hubble Space Telescope (HST) image of an extragalactic jet while the top panel shows HST images of galactic jets from young stellar objects (YSO). Microquasars (not shown) are yet another example of a (recently discovered) galactic jet. These astrophysical jets share three characteristics aside from the observed jet: (i) A spinning magnetic field; (ii) a strong magnetic field; and (iii) an accretion disk.[25] The consequence of an accretion disk is that as the disk collapses toward the central object (stellar or black hole) the disk material is heated and ionized providing a convenient source of hot plasma which is injected into the inhomogeneous magnetic field of the central attractor. The similarity of boundary conditions displayed by these example

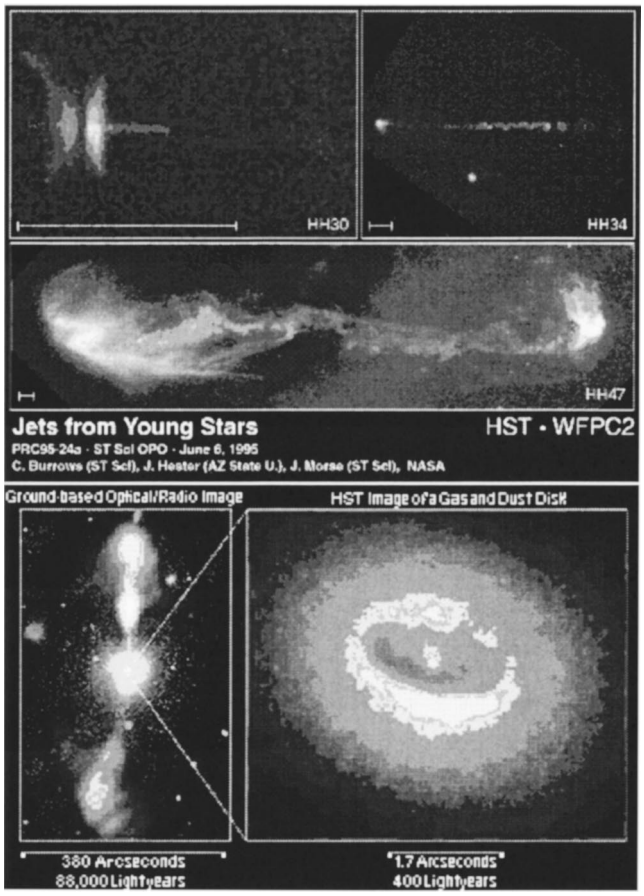

FIG. 1. Astrophysical jets as observed in young stellar objects and active galactic nuclei showing a symmetric pair of central jets surrounded by a spinning accretion disk. (Courtesy of HST.)

astrophysical jets suggests that each of these systems might be influenced by a QNC mechanism allowing these disparate systems to produce similar jets.

All these jets are observed at scales much larger than the central magnetic field, so there is little data on the structure of the magnetic field. However, we can infer from variations in the jet brightness that the acceleration region is highly compact, which is ideal for producing large ∇B-drifts.[26,27] The plasma that is injected at the magnetic equator of the accretion disk would then separate via the QNC mechanism into a heavy core of ions grouped around the equator and a hot halo of electrons that bounce vigorously around the ions. This is analogous to an ambipolar electric field that forms when an isothermal plasma is placed in a gravitational potential, only in this case, it is the mirror force plus the centrifugal barrier that plays the part of the gravitational well. The symmetry of the magnetic dipole field results in an ambipolar electric quadrupole, where the perpendicular energy of the plasma determines the potential difference between the equator and the poles.

The result of this quadrupole is the acceleration of positive particles from the equator toward the poles. For example, should the potential exceed 1.022 MV, electron-positron pairs would be formed on collisions of the electrons with the accretion disk, resulting in positrons being accelerated toward the poles. As the positron gained energy, it

would get less magnetized and eventually escape from the dipole field. (This does not occur for the electrons, because they decelerate as they move away from the equator, becoming more highly magnetized.) Such a demagnetization would be enhanced at a kink in the field, which itself may be the result of the extended electron cloud. The interaction of relativistic plasma with magnetic fields is an area of ongoing research, but the overall effect is predictable, a pair of beams of matter emanating perpendicular to the accretion plane, and accelerated to high velocity. Since nothing in our QNC model specifies the maximum perpendicular energy (as long as it is finite), one would imagine that an astrophysical instability would be driven until it saturates.

We note that the parallel electric field produced by separation of charge in a magnetic field also causes a perpendicular or polarization electric field. It is precisely because the first order drift of plasma in such a polarization electric field, $v_d = E \times B$ is perpendicular to the electric field that the plasma is not able to short out the polarization field, which is what sets up the equilibrium between the mirror force and the space charge in the first place. However, when the perpendicular field is strong enough, second order drifts, $v_{dd} = (E \times B) \times B$ *are* in the same direction as the applied electric field and the polarization field can short out the space charge. Thus the QNC mechanism saturates as some power of the space charge, which occurs before other saturation mechanisms such as demagnetization.

Scaling this second-order drift as described by Rothwell[28] to astrophysical dimensions predicted correctly that AGN's, with a 1 G field extending 1 AU in diameter, should have a jet energy of ~1 GeV, whereas YSO's should have keV jet speeds. This excellent agreement over many orders of magnitude encouraged us to build a table top laboratory experiment to produce parallel potentials using a spinning magnet and a dc plasma injector.

V. EXPERIMENTAL SETUP

We converted a 19 inch bell jar evaporator into a plasma discharge system (see Fig. 2). A Nd-B-Fe cylindrical magnet, 1 cm radius and 1 cm thick with surface field approaching 5 kG, was mounted on a stainless rod through a rotating feedthrough to a computer controlled motor. Two high voltage electrodes were mounted on either side of the magnet, each with its own high voltage power supply. Fragments of a Sylvania Cool-White fluorescent tube were used, glass side up as an x-ray detector, phosphor side up as an electron detector. A roughing pump was used to bring the pressure of the system down to a value of ~20 mTorr. A needle leak valve was used to establish higher pressures by bleeding in either nitrogen or helium gas. Several digital cameras were used to take the pictures, beginning with two 8-bit color cameras followed by two 16-bit astronomy cameras.

A. Electron injection in nitrogen plasma

When a negative potential of ~1 kV is applied to the electrode, a weak glow (in N_2) indicates that electrons are ionizing the background gas and electrons are injected into the plasma (Fig. 3). Electrons that have small pitch angles

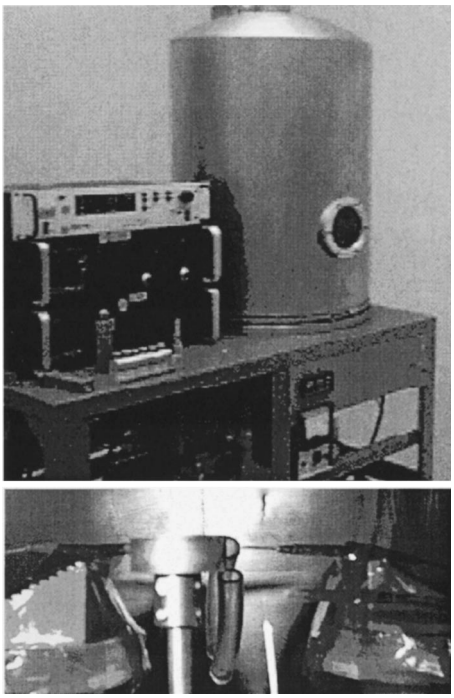

FIG. 2. The outside of the 19 inch stainless bell jar vacuum chamber (top panel) and the inside of the UAH Spinning Terrella Accelerator. See text for details.

are attracted to the grounded magnet, producing copious x-rays. Faint ''horns'' can be seen on the field lines that connect the electrode to the magnet. Electrons that have pitch angles near 90° gradient drift around behind the magnet and can be seen to the left of the magnet as a faint glow outlining the dipole field lines. The x-ray detector brightens as the voltage on the electrode is raised. Electrons that impact on the top of the magnet form a circular aurora made more visible by a light coating of phosphor dust.

The 16-bit resolution camera was able to better capture the density of electrons as they drifted around the magnet. We show the last two panels of Fig. 3 in false color, the left at 2.5 kV potential, the right at 4 kV. One artifact of the

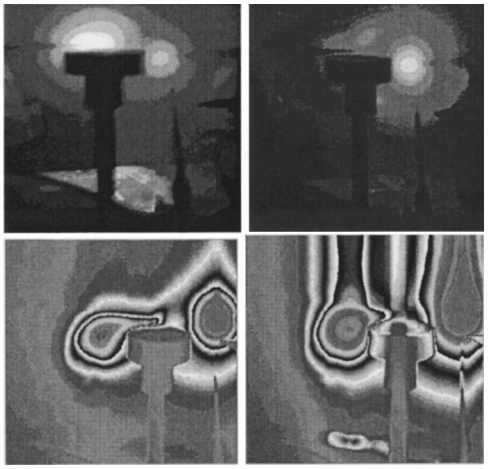

FIG. 3. First and second panel show ion and electron injection, respectively, revealing magnetic trapping of plasma. Third and fourth panels show electron injection at 2.5 kV and 4 kV, respectively, in false color.

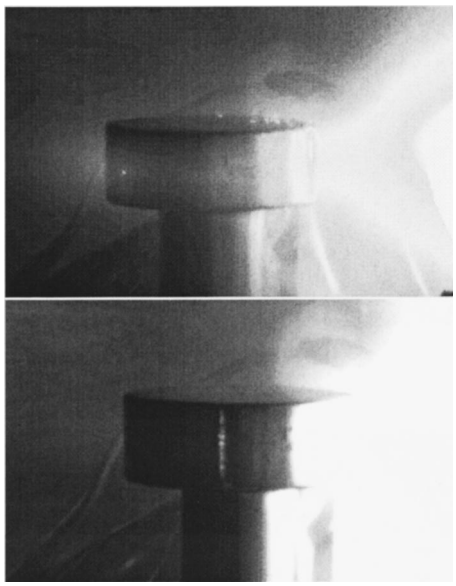

FIG. 4. Ion injection into N_2 at 50 mTorr (top panel) and 300 mTorr (bottom panel) showing magnetic trapping of plasma in a torus near the equator of the magnet.

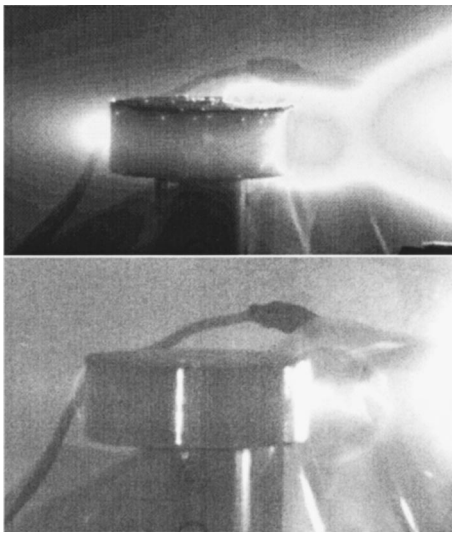

FIG. 5. Ion injection into helium at 100 mTorr (top panel) and 400 mTorr (bottom panel) showing circular plasma discharges that follow the magnetic flux tube.

digitization is the ''bleeding'' upward of the pixels as they are read from the camera. In both panels the electrode was bright enough to saturate the pixels in a small region. Note the auroral zone expands outward as the electron energy is raised. Other than slight density changes, the plasmas show no qualitative differences. Nor did spinning the magnet make much qualitative difference, though it did affect the x-ray shadow.

B. Ion injection in a nitrogen atmosphere

When we applied a positive bias to the electrode, we began injecting ions into the system. As can be seen in panel one of Fig. 3, ion injection is far brighter because inrushing electrons ionize the gas around the electrode and produce a feedback sheath effect, which in a nitrogen plasma, is a bright pink corona around the electrode. This feedback meant that a great deal of current was drawn from the power supply, and often only a few hundred volts could be established before the current limit of our power supply tripped. In the following set of pictures with positive bias, we selected a high voltage, usually $V>600$ V, and pulsed the power supply by continuously resetting it. In this way we injected ions of relatively high energy into the magnetic field.

The top panel of Fig. 4 shows a nitrogen plasma at 50 mTorr with electrodes pulsed at 600 and 1400 V. The bottom panel differs only in being at 300 mTorr. Note that at 50 mTorr, the ions can drift completely around the magnet, though the large mass of the N^+ ion means that ions are trapped only very close to the magnet. So a distinct donut or equatorial distribution can be seen. Occasionally bright spots will flare up around equator, traditionally explained as due to the potential difference between the plasma torus and grounded magnet causing a feedback ionization or sputtering hot spot. Prominent in the 50 mTorr but absent in the 300 mTorr figure are hot spots on the *top* of the magnet (and presumably, on the bottom as well). These are individual discharges lasting less than a second that are captured in the 40 s exposure. Not as well resolved (due to poor photographic technique) are the thin filaments from these discharges that form complete loops around the magnet. Since the nickel plated magnet is an equipotential, and the discharge is dc, such a filament should only be able to form if there are parallel potentials along the magnetic-field lines, symmetric about the equator. This is what is expected for the QNC.

The discharges are more obvious to the naked eye, which seems to have a better transient response. We began to explore the parameters for these circular discharges. Simultaneous injection of electrons did nothing to enhance the effect, and may, in fact, suppress it. Reducing the pressure to 20 mTorr also seemed to suppress, or ''blur'' the circular discharges. Pulsing the positive power supplies at higher voltage also had no effect, nor did spinning the magnet up to $\sim$1000 rpm. Since the trapped plasma appears very close to the magnet, it seems that the gyroradius size is important because of wall effects. We also observed that the initial discharges obtained soon after closing up the vacuum chamber were more intense. We thought the discharge might have something to do with water, and reasoned that a less massive background gas might show us gyroradius effects, so we tried helium and obtained the images described in the next section.

C. Ion injection in a helium atmosphere

Almost immediately we noticed a great intensification of the circular discharges (Fig. 5). As we raised the pressure of helium from 60 to 200 mTorr, the circular lightning became more distinct, and with further pressure increase, it reduced in frequency as well as diameter. The top panel of Fig. 5 is 100 mTorr with electrodes at 900 and 1400 V (briefly); the bottom panel is identical but at 400 mTorr. Note the many

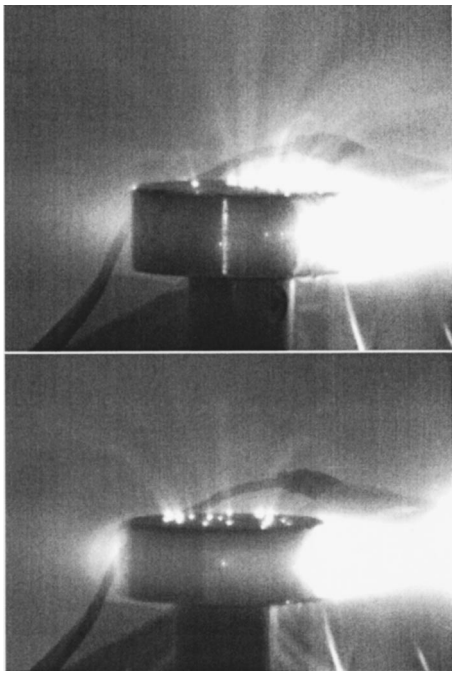

FIG. 6. Ion injection into 200 mTorr helium showing the effect of spinning the magnet (bottom) vs a stationary magnet (top panel).

discharges in the top panel, increasing in occurrence on the edge closer to the ion injector. The point discharges along the cylindrical sides of the magnet often occur in pairs, with at least one pair connected by a loop. The discharges from the top can be seen to follow larger magnetic loops. The trapped plasma produces a noticeable bright band at the equator. In the bottom panel, only two discharges are observed over the same 30 second exposure, though comparatively brighter. The larger of the two is closest to the ion injector.

The parameters show that lower pressures are more easily ionized and produce more discharges, while the higher pressures have fewer but brighter discharges. We, therefore, use 200 mTorr as a good intermediate pressure to show the effect of adjusting the other parameters. In particular, we want to know if spinning the magnet can intensify the process. Note that very little trapped plasma is visible in the higher pressure system, most probably due to the shorter scattering length preventing the ions from drifting completely around the magnet.

Both panels of Fig. 6 are taken at 200 mTorr, with 900 and 1400 V on the electrodes. The panel at the bottom shows the effect of spinning the magnet at ~1000 rpm. Note that the discharges are very evenly distributed across the magnet. The torus of trapped plasma appears more intense as well. This suggests that even as highly collisional as this plasma is, the induced electric field enhances the separation of charges and produces a more intense trapped ion plasma. Close inspection of the top panel with the stationary magnet reveals an arcade of discharges near the equatorial region at the spot where the advancing cloud of ions ∇B-drift away from the magnet.

VI. DISCUSSION

We estimate the voltage of the discharges by calculating the mean free path (MFP). The Chemical Rubber Company (CRC) handbook lists the MFP for neutral helium at standard temperature and pressure (STP) to be 27.45×10^{-6} cm. Since MFP $\propto 1/n_{\mathrm{He}}$, where n_{He} is the density, we multiplied by a factor of 7600 for a 100 mTorr pressure giving a 2 mm MFP. Now for a lightning discharge to form, the electrons in the leader of the lightning stroke must be accelerated to at least 24.5 eV before they can ionize the helium, and this must occur in less than 2 mm. This gives a value of $E_{\|}>12\,250$ V/m for an electric field. If the discharge begins at the equator and proceeds in both directions down to the magnet, the distance could be as much as 4 cm, resulting in a voltage greater than 500 V. At a density of 200 mTorr, the same calculation gives 1 kV, and at 400 mTorr, we would produce 2 kV.

However, we also note that the discharges are brightest at the magnet and fade as they approach the equator. Since our mechanism relies on an electric field $E_{\|}$ scaling as $1/r^4$, the fact that the discharges are brightest close to the magnet is consistent with our model. In addition, the electrons diverge as the flux tube expands away from the magnet, resulting in a rapid fading of the glow along the flux tube. However, a variable $E_{\|}$ does suggest that our quick calculation above be modified. If the strength of $E_{\|}$ drops below ionization threshold, we would expect the glow to cease within a scattering length or two. So if we start with the dim part of the flux tube and integrate to the brightest spot on the flux tube, one would expect the electric field to increase with some power of r^{-n}, where our quick calculation above used $n=0$. Thus it would appear that our calculation above is a lower limit for potentials generated by the system.

When we look in detail at the pressure changes, we note that the lower pressure regimes have a ''comet-like'' appearance, with a bright ''coma'' near or on the surface of the magnet, and a dim tail. The high-pressure discharges (400 mTorr), lack the presence of the coma, and the intensity of the discharge does not vary along the flux tube. The coma might be the collision of the particles with the magnet and subsequent sputtered plasma glowing more brightly than the neutral gas. Alternatively, it may be that the long tail is a secondary effect of cold accelerated ions colliding with the gas, as proposed for the POLAR/CEPPAD data. Spectroscopic or fast timing images should be able to sort out the evolution of a single discharge, but this is beyond the scope of our preliminary results.

The lack of a coma in the high pressure case may also be explained from the simple theory above. We note that a distinct ''mirror-point'' collection of hot ions occur only for mono-pitchangle particles. At high pressures, we might expect the hot ions to scatter isotropically and therefore not produce as rapidly varying radial electric field.

If the creation of the space charge can be viewed as charging a capacitor in an RC circuit, then it agrees with the observation that the discharges become less frequent and brighter as the pressure is increased. Since a voltage greater than 500 V was required experimentally to produce a dis-

charge in 200 mTorr He, we estimate that at least half of the 1400 eV of the injected ions is extracted in these discharges, in agreement with the data from space and our simple theory.

Spinning the magnet (panel two of Fig. 6) increases the corotation speed of the ions due to the additional $E\times B$-drift. In our experiment, we spun the magnet in the same sense as the ∇B-drift for ions, thereby spreading the ions more evenly around the magnet. From our model, this increased the area and hence the capacitance of the space charge, and thus permitted more charge to collect and more intense flashes for the same voltage. Note how evenly the discharges occur in the second panel as compared to the first panel of the Fig. 6. In space and astrophysical systems, the more even distribution generated by spinning also has the same effect, allowing the spatial scale of the space charge capacitor to be the size of the system itself. As we calculated for AGN blazars, this permits the longest length scale and highest acceleration potential to produce the 1 GeV astrophysical jets.

VII. CONCLUSIONS

The table top experiment results suggest that a dipole magnetic field may trap charge, which would provide support for the proposed QNC mechanism responsible for field-aligned flows observed by Earth-orbiting spacecraft. The interpretation of the observed collimated beams as induced by space charge is supported by a collisionless plasma calculation, which predicts to within a factor of two the beam to injected ion energy ratio. The robust nature of the laboratory discharges, observed over a decade of pressure change (and many more decades if extrapolated to Earth orbit) suggests that the phenomenon may be quite common in the many regimes of space and astrophysical plasmas. Consideration of a simple saturation mechanism gives the correct order-of-magnitude estimate for the jet energies of two very different scale astrophysical systems, YSO and AGN jets. Thus the energy source for many astrophysical plasma processes may turn out not to be shocks, the current favorite mechanism, but the ubiquitous parallel electric field. Future work will present a quantitative description of this vacuum magnetic capacitor and dependence of the parallel field on boundary conditions.

[1] L. R. Lyons and D. J. Williams, *Quantitative Aspects of Magnetospheric Physics* (Reidel, Dordrecht, 1984).
[2] M. Temerin, Adv. Space Res. **20**, 1025 (1995).
[3] N. A. Krall and A. W. Trivelpiece, *Principles of Plasma Physics* (San Francisco Press, San Francisco, 1986).
[4] H. Alfven and C.-G. Falthammar, *Cosmical Electrodynamics, Fundamental Principles* (Clarendon, Oxford, 1963).
[5] E. C. Whipple, Jr., J. Geophys. Res. **82**, 1525 (1977).
[6] G. J. Fishman, P. N. Bhat, R. Malozzi, J. M. Horack, T. Koshut, C. Kouveliotou, G. N. Pendelton, C. A. Meegan, R. B. Wilson, W. S. Paciesas, S. J. Goodman, and H. J. Christian, Science **264**, 1313 (1994).
[7] R. E. Ergun, C. W. Carlson, J. P. McFadden, F. S. Mozer, G. T. Delory, W. Peria, C. C. Chaston, M. Temerin, R. Elphic, R. Strangeway, R. Pfaff, C. A. Cattell, D. Klumpar, E. Shelley, W. Peterson, E. Moebius, and L. Kistler, Geophys. Res. Lett. **25**, 2025 (1998).
[8] R. B. Sheldon, H. Spence, and J. Fennell, Geophys. Res. Lett. **25**, 1617 (1998).
[9] R. B. Sheldon, ''The spinning Terrella plasma accelerator,'' in *Proceedings of the Young Faculty Research at UAH* (University of Alabama in Huntsville, Huntsville, AL, 1999), pp. 95–100.
[10] A. G. Emslie and J.-C. Henoux, Astrophys. J. **446**, 371 (1995).
[11] D. L. Williams, B. H. Mauk, R. E. McEntire, E. C. Roelof, T. P. Armstrong, B. Wilken, J. G. Roederer, S. M. Krimigis, T. A. Fritz, and L. J. Lanzerotti, Science **274**, 401 (1996).
[12] J. E. Pringle, ''Cosmogony of stellar and extragalactic jets,'' in *Astrophysical Jets: Space Telescope Science Institute Symposium Series* (Cambridge University Press, Cambridge, 1993), pp. 1–12.
[13] F. Fiore, L. La Franca, P. Giommi, M. Elvis, G. Matt, A. Comastri, S. Molendi, and I. Gioia, Mon. Not. R. Astron. Soc. **306**, L55 (1999).
[14] M. A. Uman, *Lightning* (Dover, New York, 1984).
[15] L. Knight, Planet Space Sci. **21**, 741 (1973).
[16] C. Hansen and J. Fajans, Phys. Rev. Lett. **74**, 4209 (1995).
[17] R. B. Sheldon, ''Plasmasheet convection into the inner magnetosphere during quiet conditions,'' in *Solar Terrestrial Energy Program: COSPAR Colloquia Series Vol. 5*, edited by D. N. Baker, V. O. Papitashvili, and M. J. Teague (Pergamon, New York, 1994), pp. 313–318.
[18] K. Mursula, T. Braysy, and G. Marklund, ''ULF wave activity above the ionosphere during magnetic storms,'' in 31st Scientific Assembly of COSPAR, abstracts, D0.5-0019 (1996).
[19] D. Chenette, W. Imhof, S. Petrinec, M. Schulz, J. Mobilia, J. Pronko, M. Rinaldi, J. Cladis, F. Fenrich, N. Østgaard, and M. McNab, ''Global energy-resolved x-ray images of northern aurora and their mappings to the equatorial magnetosphere,'' in *Sun-Earth Plasma Connections: Geophysical Monograph Series Vol. 109* (American Geophysical Union, Washington, D.C., 1999), pp. 65–76.
[20] R. B. Sheldon and H. E. Spence, ''A new magnetic storm model,'' in Geospace Mass and Energy Flow: Result from the International Solar-Terrestrial Physics Program, Washington, DC, 1998, edited by J. Horwitz.
[21] R. B. Sheldon, Adv. Space Res. **25**, 2347 (2000).
[22] D. C. Hamilton, G. Gloeckler, F. M. Ipavich *et al.*, J. Geophys. Res. **93**, 14343 (1988).
[23] I. A. Daglis and W. I. Axford, J. Geophys. Res. **101**, 5047 (1996).
[24] M. Grande, C. H. Perry, A. Hall, J. Fennell, and B. Wilken, Adv. Space Res. **20**, 321 (1997).
[25] S.-N. Zhang, private communication, 1999.
[26] R. Blandford, ''Present and future blazar variability (i),'' in *Blazar Continuum Variability, Conference Series, Vol. 110*, edited by H. R. Miller, J. R. Webb, and J. C. Noble (Astronomical Society of the Pacific, San Francisco, 1996), pp. 475–488.
[27] A. P. Marscher, ''Variability of the non-thermal emission in the jets of blazers (i),'' in *Blazar Continuum Variability, Conference Series, Vol. 110*, edited by H. R. Miller, J. R. Webb, and J. C. Noble (Astronomical Society of the Pacific, San Francisco, 1996), pp. 248–261.
[28] P. L. Rothwell, M. B. Silevitch, L. P. Block, and C.-G. Fälthammer, ''Single ion dynamics and multiscale phenomena,'' in *Cross-Scale Coupling in Space Plasmas*, edited by J. L. Horwitz, N. Singh, and J. L. Burch, Geophysical Monograph 93 (American Geophysical Union, Washington, D.C., 1995), pp. 151–154.